UNDER REVIEW

RESCIENCE C

Replication / Non-linear dynamics

[Re] Periodic forcing of a limit-cycle oscillator: Fixed points, Arnold tongues, and the global organization of bifurcations

Jacob K. Harvey[1,2], Lucas Philipp[1,2], and Kiri Stern[1,2]

[1]Quantitative Life Sciences, McGill University, 550 Sherbrooke W., Montréal (QC), H3A 1E3, Canada – [2]Equal contributions

Edited by (Editor)

Received –

Published –

DOI –

Abstract The effects of periodic forcing of a nonlinear limit-cycle oscillator with varying relaxation rates may provide insight into the real behaviour of oscillatory cardiac tissue. Here we successfully replicate a mathematical model by Glass & Sun (1994) and analyze its dynamical behaviour. We numerically study the geometry of phase-locking regions as the rate of return to the limit cycle, the stimulus intensity, and the time interval between stimulations are varied. Furthermore, we algebraically compute the instability boundary along the 1:0 and 1:1 (period #: cycle #) phase-locking regions and show agreement with our numerical results.

1 Introduction

Certain physiological mechanisms that drive biological processes follow periodic synchronizations or rhythms. Examples of such phenomena include our heartbeats, the circadian rhythm, the menstrual cycle, hormone regulation, oscillating neurons, and more. While disruption or dis-regulation of proper biological rhythms has been associated with disease, induced perturbations to these oscillating systems (via a pacemaker or administration of therapeutic drugs) can reset the dynamics back to normal states[1].

In 1994, Glass & Sun[2] mathematically approximated the effects of periodic pulsatile stimulations to cardiac oscillations using the Poincaré oscillator model. The oscillator is a 2D vector in an abstract polar coordinate (r, ϕ) state space with $0 \leq \phi \leq 1$, that evolves with time according to:

$$\frac{\partial r}{\partial t} = kr(1-r) \tag{1}$$

$$\frac{\partial \phi}{\partial t} = 1 \tag{2}$$

where r is the radial coordinate, ϕ is the angular coordinate, and k is the relaxation rate representing the rate of return to the circular limit cycle located at $r = 1$. This evolution is periodically interrupted by a horizontal perturbation of magnitude b every τ units of time. Initially, a point (r_i, ϕ_i) is perturbed horizontally by an amount b to (r'_i, ϕ'_i), then (r'_i, ϕ'_i) is evolved according to the differential equations above for a time τ arriving at the point (r_{i+1}, ϕ_{i+1}) (see Fig 1). We can solve these differential equations explicitly to get a 2-dimensional map relating the perturbation points (r'_i, ϕ'_i) to the next point at time τ after relaxation, (r_{i+1}, ϕ_{i+1}).

$$r_{i+1} = \frac{r'_i}{(1-r'_i)e^{-k\tau} + r'_i} \tag{3}$$

Copyright © 2022 J. K. Harvey, L. Philipp, and K. Stern, released under a Creative Commons Attribution 4.0 International license.
Correspondence should be addressed to Lucas Philipp (lucas.philipp@mail.mcgill.ca)
The authors have declared that no competing interests exist.
Code is available at https://github.com/jkharv/poincare_oscillator. – SWH .

$$\mathrm{mod}\{\phi_{i+1} = \phi'_i + \tau, 1\} \tag{4}$$

Glass & Sun[2] studied the organization of regions in (b, τ) space for which a stable periodic oscillation and fixed point exists. These regions, called phase-locking regions or "Arnold tongues", depend on the relaxation rate k. They are annotated according to the number of stimuli per period (period #) and the number of complete revolutions in phase (cycle #) before returning to the fixed point ϕ.

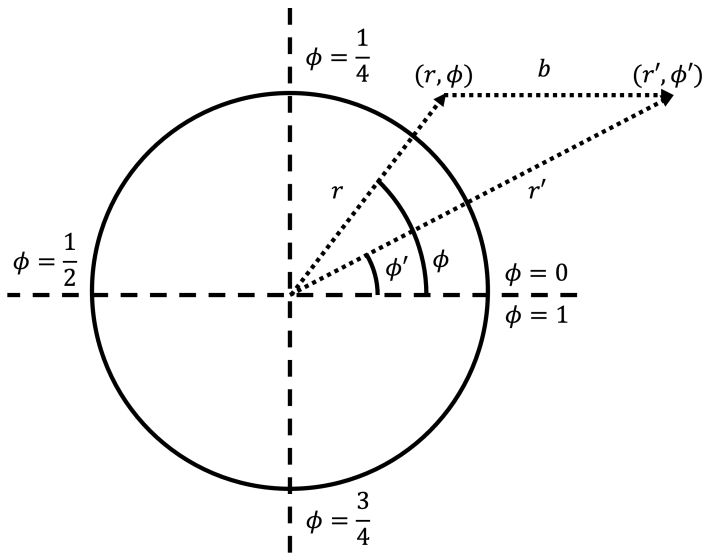

Figure 1. A diagram of the oscillator, as seen in Figure 1 from Glass & Sun [2].

In this study, we successfully replicate the complex dynamical behaviour observed by Glass & Sun (1994)[2] resulting from only two uncoupled ordinary differential equations and periodic forcing. This replication study is significant because, firstly, it numerically describes how the finite relaxation rate back to the limit cycle affects the complex organization of the phase-locking regions and, secondly, because it analytically clarifies aspects of the instability boundary along the 1:0 and 1:1 (period #: cycle #) phase-locking regions in the infinite relaxation limit ($k \to \infty$).

2 Numerical Methods

We successfully replicated the results of Glass & Sun (1994)[2] in the programming language Julia (version 1.7.2). To overcome numerical inaccuracy issues, we use a version of the system[3] transformed into Cartesian coordinates with the form (x_i, y_i) using equations (3) & (4):

$$x_{i+1} = \frac{(x_i + b)\cos(2\pi\tau) - y_i \sin(2\pi\tau)}{(1 - r'_i)e^{-k\tau} + r'_i} \tag{5}$$

$$y_{i+1} = \frac{y_i \cos(2\pi\tau) + (x_i + b)\sin(2\pi\tau)}{(1 - r'_i)e^{-k\tau} + r'_i} \tag{6}$$

where

$$r'_i = [(x_i + b)^2 + y_i^2]^{1/2}$$

This resolves the issue of round-off errors when $r_i \approx 1$, $b \approx 1$, and $\phi_i \approx 0.5$. In order to visually compare our results with the original paper, we then convert the Cartesian coordinates back into Polar coordinates.

We use initial values ($x = 1$, $y = 0$) equivalent to ($r = 1$, $\phi = 0$) for $k = 50 \approx \infty$ to replicate Figure 2 of Glass & Sun (1994)[2]. The model is simulated over a period of 800 time-steps, however, we only consider the periodic cycles after a 500 transient time had passed.

We compare the global organization of phase-locking regions for different values of b and τ at $k = 50 \approx \infty$, $k = 10$, and $k = 1$. For k set as 10 or 1, we use the initial points ($x = -0.3081$, $y = 0.9514$) which correspond approximately to the arbitrarily chosen initial states ($r = 1$, $\phi = 0.3$) of the original paper. Furthermore, to investigate the dynamics at specific regions of the phase-locking zones, we produce Figures 2d and 2e, zoomed in at $\tau = 0.25$ and $b = 1$.

Figure 2 shows the phase-locking zones between the number of stimuli per period (denoted *period n*) for 1 cycle, in an $n : 1$ ratio. This differs from Glass & Sun (1994)[2] where τ was set between 0 and 2. We chose τ between 1 and 2 as it is simply a reflection of the image at τ between 0 and 1.

3 Analytical Results

Here, we analytically calculate the period-1 instability boundary in the immediate relaxation limit ($k \to \infty$). $k \to \infty$ is called the immediate relaxation limit as the system returns (in the radial direction) to the limit cycle at $r = 1$ immediately after the perturbation; all time evolutions occur on the unit circle and the 2D map reduces to a 1D map described by $\phi_{i+1}(\phi_i, b, \tau)$. The period-1 instability boundary is determined by setting $\phi_{i+1} = \text{mod}\{\phi_i, 1\}$ (period-1 condition, see equation 4) and $|\frac{\partial \phi_{i+1}}{\partial \phi_i}| > 1$ (instability condition). $|\frac{\partial \phi_{i+1}}{\partial \phi_i}| > 1$ represents small deviations from the fixed point becoming larger after applications of the 1D map (Strogatz, 2000[4]). After a few standard manipulations, as described in the Appendix section 4.1, we find for the 1D map $\phi_{i+1}(\phi_i, b, \tau)$ the following result; and calculate its derivative.

$$\phi_{i+1} = \begin{cases} \frac{1}{2\pi} \arccos(\frac{b + r\cos(\phi 2\pi)}{\sqrt{r^2 + b^2 + 2rb\cos(\phi 2\pi)}}) + \tau & 0 \leq \phi_i \leq 1/2 \\ -\frac{1}{2\pi} \arccos(\frac{b + r\cos(\phi 2\pi)}{\sqrt{r^2 + b^2 + 2rb\cos(\phi 2\pi)}}) + 1 + \tau & 1/2 \leq \phi_i \leq 1 \end{cases} \tag{7}$$

The derivative is found to be:

$$\frac{\partial \phi_{i+1}}{\partial \phi_i} = \frac{1 + b\cos(2\pi\phi_i)}{1 + b^2 + 2b\cos(2\pi\phi_i)} \tag{8}$$

The general strategy to compute the instability is to set $\frac{\partial \phi_{i+1}}{\partial \phi_i} = \pm 1$ which will give an equation for $b(\phi_i)$. $b(\phi_i)$ can be substituted into $\phi_{i+1}(\phi_i, b, \tau)$; and setting $\phi_{i+1} = \phi_i$ (period-1 condition) gives $\phi_i(\tau)$. Finally, $\phi_i(\tau)$ is substituted into $b(\phi_i)$ resulting in the period-1 ($k \to \infty$) instability boundary $b(\tau)$.
We start by setting $\frac{\partial \phi_{i+1}}{\partial \phi_i} = 1$.

$$1 = \frac{1 + b\cos(2\pi\phi_i)}{1 + b^2 + 2b\cos(2\pi\phi_i)} \tag{9}$$

$$b = -\cos(2\pi\phi_i) \tag{10}$$

This is then substituted in Eq. 7, and the period-1 condition is applied.

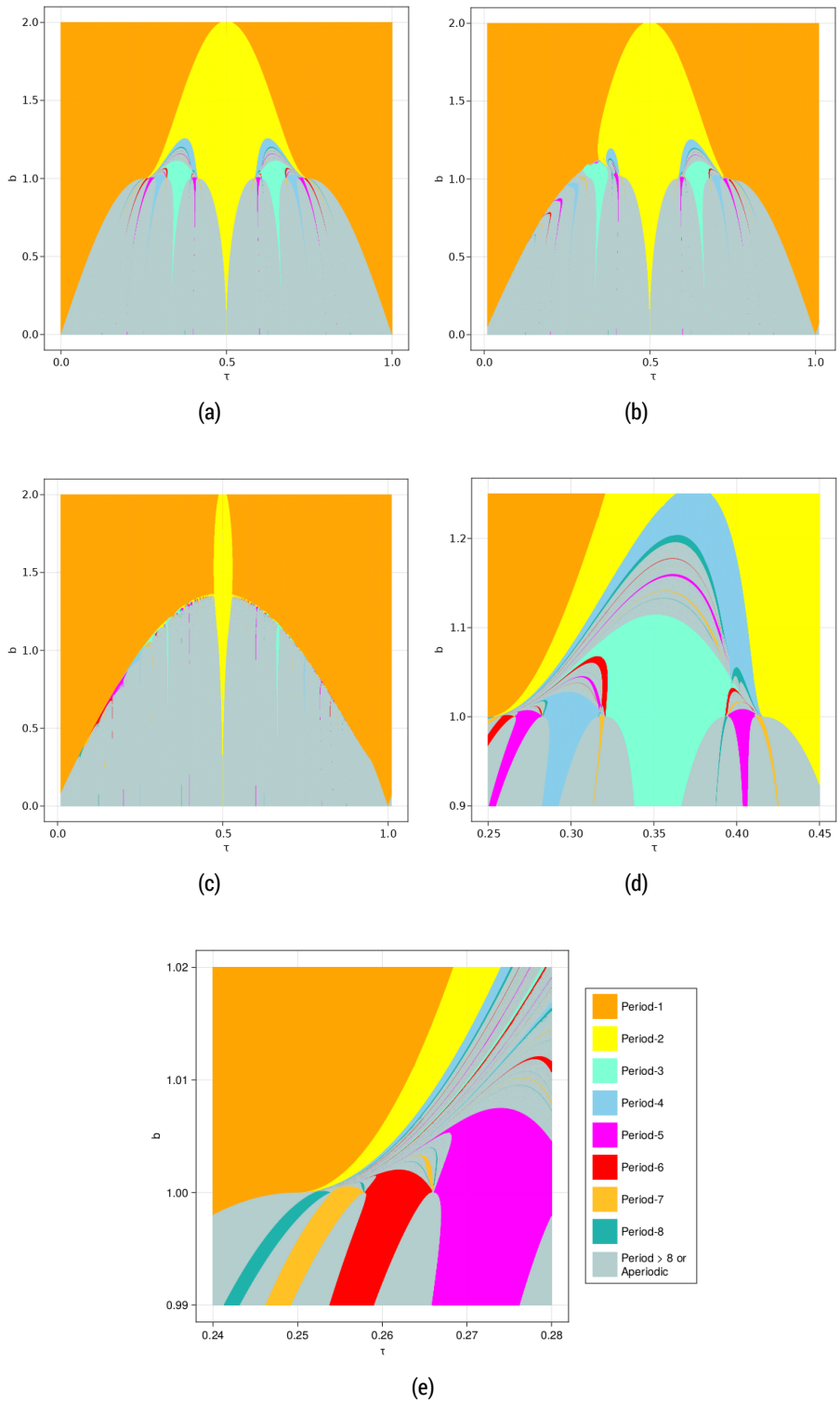

Figure 2. Global organization of phase-locking zones of the periodically forced oscillator for different relaxation rate. We demonstrate the organization of the phase-locking zones for (a) $k = 50 \approx \infty$; (b) $k = 10$; (c) $k = 1$; (d) $k = 50$ at increased resolution at point $\tau = 0.25$ and $b = 1.0$; (e) $k = 50$ at increased resolution at point $\tau = 0.35$ and $b = 1$. We show the $n : 1$ locked period-cycles for different frequencies of stimulus τ and magnitude of stimulus b, as aforementioned in the text. We were able to successfully reproduce corresponding Figure 2, Figure 5a and Figure 5b of the original study. Despite the expected minor differences, our results follow the same overall patterns.

For $0 \leq \phi_i \leq 1/2$, we have:

$$\phi_{i+1} = \phi_i = \frac{1}{2\pi} \arccos(\frac{b + \cos(\phi_i 2\pi)}{\sqrt{1 + b^2 + 2b\cos(\phi_i 2\pi)}}) + \tau \tag{11}$$

$$= \frac{1}{2\pi} \arccos(0) + \tau = 1/4 + \tau. \tag{12}$$

Since $1/4 + \tau = \phi_{i+1} = \phi_i \leq 1/2$, this implies $\tau \leq 1/4$.
For $1/2 \leq \phi_i \leq 1$, we have:

$$\phi_{i+1} = \phi_i = -\frac{1}{2\pi} \arccos(\frac{b + \cos(\phi_i 2\pi)}{\sqrt{1 + b^2 + 2b\cos(\phi_i 2\pi)}}) + 1 + \tau \tag{13}$$

$$= -\frac{1}{2\pi} \arccos(0) + 1 + \tau = 3/4 + \tau. \tag{14}$$

Since $1/2 \leq 3/4 + \tau = \phi_{i+1} = \phi_i$, this implies $\text{mod}\{-1/4, 1\} \leq \tau$, which in turn implies $\tau \geq 3/4$.
Eq. 10 can be re-written as:

$$\begin{aligned} b &= -\cos(2\pi\phi_i) \\ &= -\cos(2\pi(1/4 + \tau)) && 0 \leq \phi_i \leq 1/2 \\ &= \sin(2\pi\tau) && \tau \leq 1/4 \end{aligned} \tag{15}$$

or as

$$\begin{aligned} b &= -\cos(2\pi\phi_i) \\ &= -\cos(2\pi(3/4 + \tau)) && 1/2 \leq \phi_i \leq 1 \\ &= -\sin(2\pi\tau) && \tau \geq 3/4 \end{aligned} \tag{16}$$

In summary,

$$b = |\sin(2\pi\tau)| \tag{17}$$

for $\tau \leq 1/4$ and $\tau \geq 3/4$.

We can also set $\frac{\partial \phi_{i+1}}{\partial \phi_i} = -1$ to determine other instability boundaries:

$$\begin{aligned} -1 &= \frac{1 + b\cos(2\pi\phi_i)}{1 + b^2 + 2b\cos(2\pi\phi_i)} \\ 0 &= 2 + 3b\cos(2\pi\phi_i) + b^2 \\ \frac{-b^2 - 2}{3b} &= \cos(2\pi\phi_i) \end{aligned} \tag{18}$$

The phase response curve for this instability is then:

$$\begin{aligned} \phi_{i+1} = \phi_i &= \frac{1}{2\pi} \arccos(\frac{b + \frac{-b^2-2}{3b}}{\sqrt{1 + b^2 + 2b\frac{-b^2-2}{3b}}}) + \tau \\ 2\pi(\phi_i - \tau) &= \arccos(\frac{2\sqrt{1/3 * (b^2 - 1)}}{b}) \end{aligned} \tag{19}$$

We make use of the identity $\arccos(x) = \arcsin(\sqrt{1 - x^2})$, which holds for $b > 1$, with $x = \frac{2\sqrt{1/3*(b^2-1)}}{b}$, in order to exploit the law of sines. $\sqrt{1 - x^2}$ is then $\sqrt{1 - \frac{4(b^2-1)}{3b^2}} = \sqrt{\frac{3b^2 - 4b^2 + 4}{3b^2}} = \sqrt{\frac{-b^2+4}{3b^2}}$. $2\pi(\phi_i - \tau) = \arcsin(\sqrt{\frac{-b^2+4}{3b^2}})$ so $\phi_i = \tau + \frac{1}{2\pi}\arcsin(\sqrt{\frac{-b^2+4}{3b^2}})$, which agrees with Section C of Glass & Sun[2].

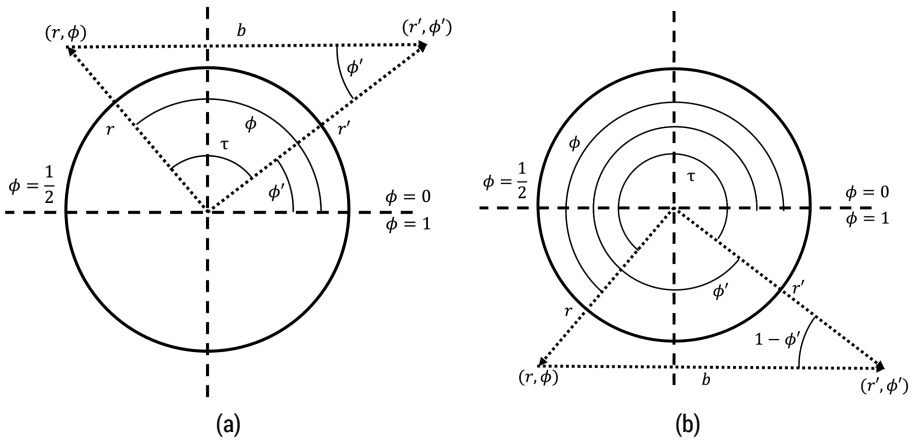

Figure 3. For the period-1 cycle, we can write (a) $\tau = \phi_i - \phi_i'$ for $0 \leq \phi \leq 1/2$ and (b) $\tau = 1 - (\phi_i' - \phi_i)$ for $1/2 \leq \phi \leq 1$.

In order to proceed, we refer to the geometry of the period-1 cycle. Referring to Fig. 3, the law of sines gives $\frac{\sin(2\pi\tau)}{b} = \frac{\sin(2\pi\phi_i')}{r_i} = \frac{\sin(2\pi(\phi_i - \tau))}{r_i}$ for $0 \leq \phi \leq 1/2$ and $\frac{\sin(2\pi\tau)}{b} = \frac{\sin(2\pi(1-\phi_i'))}{r_i} = -\frac{\sin(2\pi\phi_i')}{r_i} = -\frac{\sin(2\pi(1+\phi_i-\tau))}{r_i} = -\frac{\sin(2\pi(\phi_i-\tau))}{r_i}$ for $1/2 \leq \phi \leq 1$. Note $r_i = 1$ for $k \to \infty$. This can be used to simplify:

$$
\begin{aligned}
2\pi(\phi_i - \tau) &= \arcsin\left(\sqrt{\frac{-b^2+4}{3b^2}}\right) \\
\pm\frac{\sin(2\pi\tau)}{b} &= \sin\left(\arcsin\left(\sqrt{\frac{-b^2+4}{3b^2}}\right)\right) \\
\left(\pm\frac{\sin(2\pi\tau)}{b}\right)^2 &= \frac{-b^2+4}{3b^2} \\
b &= \sqrt{4 - 3\sin^2(2\pi\tau)}
\end{aligned}
\tag{20}
$$

In the Appendix section 4.2, we check if there are any restrictions on τ for which $b = \sqrt{4 - 3\sin^2(2\pi\tau)}$ is not a period-1 instability boundary. We find $b = \sqrt{4 - 3\sin^2(2\pi\tau)}$ holds true only for $1/4 < \tau < 3/4$.

Furthermore, we numerically simulate the period-1 instability boundary and overlay it with the phase-locking zones (see Fig. 4).

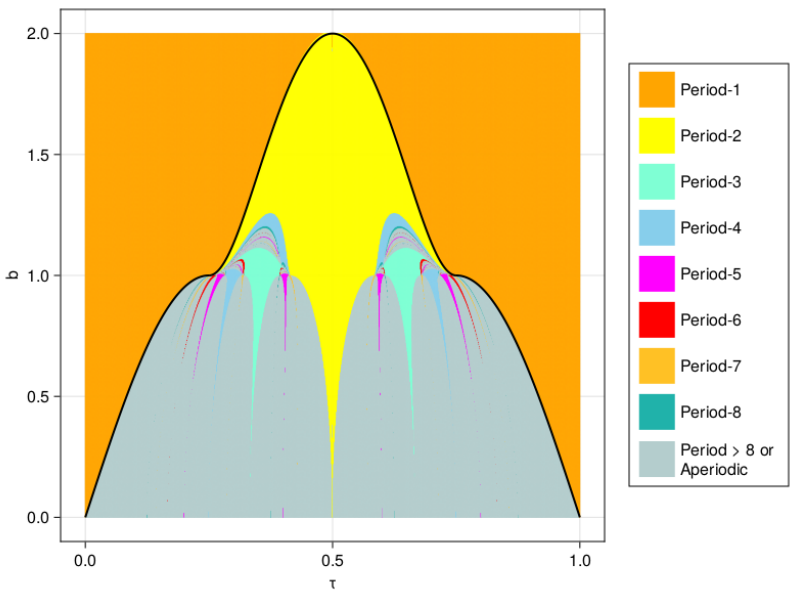

Figure 4. Phase-locking zones for the oscillator, $k = 50$, with $k \to \infty$ period-1 instability boundaries $b = |\sin(2\pi\tau)|$ ($\tau \leq 1/4$, $\tau \geq 3/4$) and $b = \sqrt{4 - 3\sin^2(2\pi\tau)}$ ($1/4 < \tau < 3/4$) in black. The grey region labelled aperiodic could include stable cycles of period nine or greater, or truly aperiodic dynamics.

Figure 4 compares the analytically calculated period-1 instability boundaries with numerical simulations results from Section 2. We observe quantitative agreement between period-1 instability boundaries determined by both methods, taking into consideration the domain restrictions on τ for Eq. 17 and Eq. 20. However, it should be noted that these calculations do not reveal the cycle number for either instability boundary.

4 Conclusion

Periodic rhythms are fundamental in driving certain biological processes. Understanding the complex dynamics arising from periodic perturbations using a simple mathematical model is an important first step towards understanding the underlying physiology in oscillatory cardiac tissue, which in turn may eventually lead to improved treatments for diseases involving rhythmic dis-regulation.

We successfully replicated the dynamics observed by Glass & Sun[2] of a periodically forced Poincaré oscillator model. Specifically, the geometry of the phase-locking regions for varying stimulus intensities, time interval between stimulations, and rate of return to the limit cycle, is reproduced numerically. In addition, the period-1 instability boundary in the immediate relaxation limit is calculated analytically and is found to agree with both our numerical results and the results presented in the original study by Glass & Sun[2]. We clarify the mathematical origin of domain restrictions on τ for Eq. 17 and Eq. 20. This is significant because without accounting for domain restrictions on τ, analytic calculations would predict certain instability boundaries that do not exist.

References

1. L. Glass. "Synchronization and rhythmic processes in physiology." In: **Nature** 410 (2001), pp. 277–284.

2. L. Glass and J. Sun. "Periodic forcing of a limit-cycle oscillator: Fixed points, Arnold tongues, and the global organization of bifurcations." In: **Physical Review. E, Statistical Physics, Plasmas, Fluids, and Related Interdisciplinary Topics; (United States)** 50:6 (Dec. 1994). DOI: 10.1103/PhysRevE.50.5077. URL: https://www.osti.gov/biblio/6785546.
3. P. Langfield, W. L. C. Façanha, B. Oldeman, and L. Glass. "Bifurcations in a Periodically Stimulated Limit Cycle Oscillator with Finite Relaxation Times." In: **SIAM Journal on Applied Dynamical Systems** 16.2 (2017), pp. 1045–1069. DOI: 10.1137/16M1082391. eprint: https://doi.org/10.1137/16M1082391. URL: https://doi.org/10.1137/16M1082391.
4. S. H. Strogatz. **Nonlinear Dynamics and Chaos: With Applications to Physics, Biology, Chemistry and Engineering**. Westview Press, 2000, p. 356.

4.1 1D Map in the Immediate Relaxation Limit and its Derivative

We seek a function $\phi_{i+1}(\phi_i, b, \tau)$ describing the system's dynamics in the limit $k \to \infty$. Using the law of cosines and noting $\angle rb = \pi - \phi 2\pi$ (see Fig. 1), the radial coordinate $r'(r, \phi, b)$ after perturbation is:

$$r' = \sqrt{r^2 + b^2 - 2rb\cos(\pi - \phi 2\pi)} \tag{S1}$$

$$= \sqrt{r^2 + b^2 + 2rb\cos(\phi 2\pi)}. \tag{S2}$$

Again, using the law of cosines, the angular coordinate $\phi'(r, \phi, b)$ after perturbation is $r = \sqrt{r'^2 + b^2 - 2r'b\cos(\phi' 2\pi)}$. Then

$$\cos(\phi' 2\pi) = \frac{r^2 + b^2 + 2rb\cos(\phi 2\pi) + b^2 - r^2}{2r'b} \tag{S3}$$

$$= \frac{b + r\cos(\phi 2\pi)}{\sqrt{r^2 + b^2 + 2rb\cos(\phi 2\pi)}} \tag{S4}$$

$$\phi' = \frac{1}{2\pi}\arccos\left(\frac{b + r\cos(\phi 2\pi)}{\sqrt{r^2 + b^2 + 2rb\cos(\phi 2\pi)}}\right) \tag{S5}$$

where Eq. S2 is used in lines S3 and S4. However, $\arccos(\cos(2\pi\phi')) = 2\pi\phi'$ only if $0 \leq \phi' \leq 1/2$. This is because arccosine only inverts the first half-period of cosine function between 0 to π. For $1/2 \leq \phi' \leq 1$, we note that $-\arccos(\cos(2\pi\phi')) + 2\pi = 2\pi\phi'$. So over the complete range of possible perturbed phases, we have:

$$\phi' = \begin{cases} \frac{1}{2\pi}\arccos\left(\frac{b+r\cos(\phi 2\pi)}{\sqrt{r^2+b^2+2rb\cos(\phi 2\pi)}}\right) & 0 \leq \phi' \leq 1/2 \\ -\frac{1}{2\pi}\arccos\left(\frac{b+r\cos(\phi 2\pi)}{\sqrt{r^2+b^2+2rb\cos(\phi 2\pi)}}\right) + 1 & 1/2 \leq \phi' \leq 1 \end{cases}. \tag{S6}$$

Integrating the angular differential equation is trivial: $\phi_{i+1} = \mathrm{mod}\{\phi'_i + \tau, 1\}$ (see equation 4), which adds τ to the above piecewise equation.

$$\phi_{i+1} = \begin{cases} \frac{1}{2\pi}\arccos\left(\frac{b+r\cos(\phi 2\pi)}{\sqrt{r^2+b^2+2rb\cos(\phi 2\pi)}}\right) + \tau & 0 \leq \phi' \leq 1/2 \\ -\frac{1}{2\pi}\arccos\left(\frac{b+r\cos(\phi 2\pi)}{\sqrt{r^2+b^2+2rb\cos(\phi 2\pi)}}\right) + 1 + \tau & 1/2 \leq \phi' \leq 1 \end{cases} \tag{S7}$$

Note that since the perturbations are horizontal, if $0 \leq \phi \leq 1/2$, then $0 \leq \phi' \leq 1/2$; and if $1/2 \leq \phi \leq 1$, then $1/2 \leq \phi' \leq 1$ (i.e. the perturbation never causes the system to cross the x-axis). For $b < 1$, as τ is increased from 0, the phase response curve $(\phi_{i+1}(\phi_i))$ intersects the line $\phi_{i+1} = \phi_i$ tangentially (see Figure S1). Hence, we conclude that for $b < 1$, the type of bifurcation for the period-1 instability boundary is a tangent bifurcation.

It is useful to rewrite $\phi_{i+1}(\phi_i, b, \tau)$ in a different form, which makes it easier to calculate the derivative $\frac{\partial \phi_{i+1}}{\partial \phi_i}$. We begin by noting that $\arccos(x) = \cot^{-1}(\frac{x}{\sqrt{1-x^2}})$ for $|x| < 1$ which is always satisfied for any ϕ, b, r, if $x = \frac{b+r\cos(\phi_i 2\pi)}{\sqrt{r^2+b^2+2rb\cos(\phi_i 2\pi)}}$. Then,

$$\frac{x}{\sqrt{1-x^2}} = \frac{\frac{b+r_i\cos(\phi_i 2\pi)}{\sqrt{r_i^2+b^2+2r_i b\cos(\phi_i 2\pi)}}}{\sqrt{1-\left(\frac{b+r_i\cos(\phi_i 2\pi)}{\sqrt{r_i^2+b^2+2r_i b\cos(\phi_i 2\pi)}}\right)^2}} \qquad r_i = 1$$

$$= \frac{b + \cos(2\pi\phi_i)}{\sin(2\pi\phi_i)}$$

$$= b\csc(2\pi\phi_i) + \cot(2\pi\phi_i) \tag{S8}$$

Which allows us to simplify the 1D map to,

$$\phi_{i+1} = \begin{cases} \frac{1}{2\pi}\cot^{-1}(b\csc(2\pi\phi_i) + \cot(2\pi\phi_i)) + \tau & 0 \leq \phi_i \leq 1/2 \\ -\frac{1}{2\pi}\cot^{-1}(b\csc(2\pi\phi_i) + \cot(2\pi\phi_i)) + \tau + 1 & 1/2 \leq \phi_i \leq 1 \end{cases}. \tag{S9}$$

The derivative is calculated directly using the chain rule.

$$\begin{aligned}
\phi_{i+1} &= \phi_i' + \tau \\
&= \frac{1}{2\pi}\cot^{-1}(b\csc(2\pi\phi_i) + \cot(2\pi\phi_i)) + \tau \\
\frac{\partial\phi_{i+1}}{\partial\phi_i} &= \frac{1}{2\pi}\frac{-\frac{\partial(b\csc(2\pi\phi_i)+\cot(2\pi\phi_i))}{\partial\phi_i}}{1+(b\csc(2\pi\phi_i)+\cot(2\pi\phi_i))^2} \\
&= \frac{1+b\cos(2\pi\phi_i)}{\sin^2(2\pi\phi_i)+\cos^2(2\pi\phi_i)+b^2+2b\cos(2\pi\phi_i)} \\
&= \frac{1+b\cos(2\pi\phi_i)}{1+b^2+2b\cos(2\pi\phi_i)}
\end{aligned} \tag{S10}$$

4.2 Restrictions on τ for the period-1 instability boundary $b = \sqrt{4 - 3\sin^2(2\pi\tau)}$

Next we check if there are any restrictions on τ for which $b = \sqrt{4 - 3\sin^2(2\pi\tau)}$ is not a period-1 instability boundary. Using the identity $\sin^2(2\pi\tau) + \cos^2(2\pi\tau) = 1$ and solving for τ we find:

$$b = \sqrt{4 - 3(1 - \cos^2(2\pi\tau))} \tag{S11}$$

$$\tau = \frac{1}{2\pi}\arccos(\pm\sqrt{(b^2-1)/3}). \tag{S12}$$

Since $\arccos(\cos(2\pi\tau)) = 2\pi\tau$ only if $0 \le \tau \le 1/2$ and $-\arccos(\cos(2\pi\tau)) + 2\pi = 2\pi\tau$, for $1/2 \le \tau \le 1$, we can write:

$$\tau = \begin{cases} \frac{1}{2\pi}\arccos(\pm\sqrt{(b^2-1)/3}) & 0 \le \tau \le 1/2, 0 \le \phi_i \le 1/2 \\ -\frac{1}{2\pi}\arccos(\pm\sqrt{(b^2-1)/3}) + 1 & 1/2 \le \tau \le 1, 1/2 \le \phi_i \le 1 \end{cases} \tag{S13}$$

Note that $0 \le \tau \le 1/2$ implies $0 \le \phi_i \le 1/2$ for the period-1 cycle, which can be checked using $\tau = \phi_i - \phi_i'$ and $\phi_i' < \phi_i$. Similarly $1/2 \le \tau \le 1$ implies $1/2 \le \phi \le 1$ which can be checked using $\tau = 1 - (\phi_i' - \phi_i)$ and $\phi_i' > \phi_i$.

Combing this result with the phase response curve $\phi_{i+1}(\phi_i)$, we get:

$$\phi_{i+1} = \begin{cases} \frac{1}{2\pi}\arccos(\frac{b+\cos(\phi_i 2\pi)}{\sqrt{1+b^2+2b\cos(\phi_i 2\pi)}}) + \frac{1}{2\pi}\arccos(\pm\sqrt{(b^2-1)/3}) & 0 \le \phi_i \le 1/2 \\ -\frac{1}{2\pi}\arccos(\frac{b+\cos(\phi_i 2\pi)}{\sqrt{1+b^2+2b\cos(\phi_i 2\pi)}}) - \frac{1}{2\pi}\arccos(\pm\sqrt{(b^2-1)/3}) + 2 & 1/2 \le \phi_i \le 1. \end{cases} \tag{S14}$$

However, when $1 \le b$, the period-1 condition $\phi_{i+1} = \mathrm{mod}\{\phi_i' + \tau, 1\}$ at the instability boundary $\frac{\partial\phi_{i+1}}{\partial\phi_i} = -1$, is satisfied only for Eq S15 and not for Eq S16.

$$\tau = \begin{cases} \frac{1}{2\pi}\arccos(-\sqrt{(b^2-1)/3}) & 0 \le \phi_i \le 1/2 \\ -\frac{1}{2\pi}\arccos(-\sqrt{(b^2-1)/3}) + 1 & 1/2 \le \phi_i \le 1 \end{cases} \tag{S15}$$

$$\tau = \begin{cases} \frac{1}{2\pi}\arccos(+\sqrt{(b^2-1)/3}) & 0 \le \phi_i \le 1/2 \\ -\frac{1}{2\pi}\arccos(+\sqrt{(b^2-1)/3}) + 1 & 1/2 \le \phi_i \le 1 \end{cases} \tag{S16}$$

At the $\frac{\partial\phi_{i+1}}{\partial\phi_i} = -1$ instability boundary, the phase must be a solution of $0 = 2 + 3b\cos(2\pi\phi_i) + b^2$:

$$0 = \begin{cases} \phi_i - \mathrm{mod}\{\frac{1}{2\pi}\arccos(\frac{b+\cos(\phi_i 2\pi)}{\sqrt{1+b^2+2b\cos(\phi_i 2\pi)}}) + \frac{1}{2\pi}\arccos(-\sqrt{(b^2-1)/3}), 1\} & 0 \le \phi_i \le 1/2 \\ \phi_i - \mathrm{mod}\{-\frac{1}{2\pi}\arccos(\frac{b+\cos(\phi_i 2\pi)}{\sqrt{1+b^2+2b\cos(\phi_i 2\pi)}}) - \frac{1}{2\pi}\arccos(-\sqrt{(b^2-1)/3}) + 2, 1\} & 1/2 \le \phi_i \le 1 \end{cases} \tag{S17}$$

$$0 = \begin{cases} \phi_i - \mathrm{mod}\{\frac{1}{2\pi}\arccos(\frac{b+\cos(\phi_i 2\pi)}{\sqrt{1+b^2+2b\cos(\phi_i 2\pi)}}) + \frac{1}{2\pi}\arccos(+\sqrt{(b^2-1)/3}), 1\} & 0 \leq \phi_i \leq 1/2 \\ \phi_i - \mathrm{mod}\{-\frac{1}{2\pi}\arccos(\frac{b+\cos(\phi_i 2\pi)}{\sqrt{1+b^2+2b\cos(\phi_i 2\pi)}}) - \frac{1}{2\pi}\arccos(+\sqrt{(b^2-1)/3}) + 2, 1\} & 1/2 \leq \phi_i \leq 1 \end{cases} \tag{S18}$$

The equation S17 is satisfied at the ϕ_i equal to the ϕ_i solutions of $0 = 2 + 3b\cos(2\pi\phi_i) + b^2$ while the equation S18 is satisfied for other ϕ_i values of the $\frac{\partial\phi_{i+1}}{\partial\phi_i} = -1$ instability boundary (see Fig S2 and Fig S3). Therefore, we reject Eq.(S16) as a solution to $\cos^2(2\pi\tau) = (b^2-1)/3$, which means $\cos(2\pi\tau) = -\sqrt{(b^2-1)/3}$ effectively restricts the period-1 instability boundary $b = \sqrt{4 - 3\sin^2(2\pi\tau)}$ to $1/4 < \tau < 3/4$, (see Fig 4).

5 Supplementary Figures

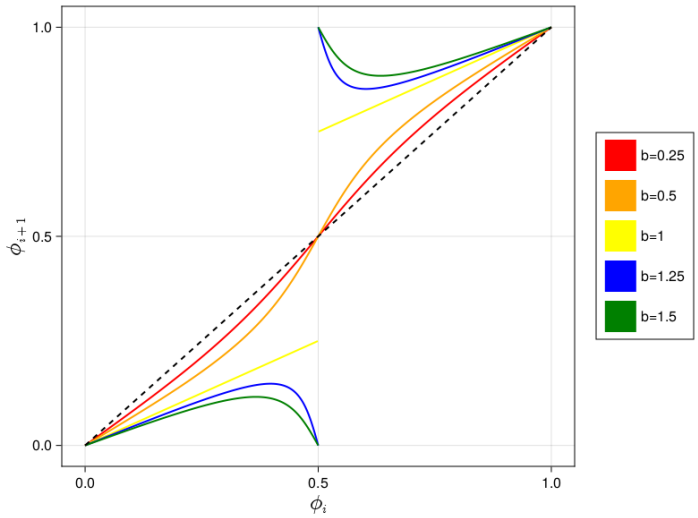

Figure S1. Phase response curves $\phi_{i+1}(\phi_i)$, Eq. S7, for $k \to \infty$ and $\tau = 0$. The dashed line is the period-1 line where $\phi_{i+1} = \phi_i$.

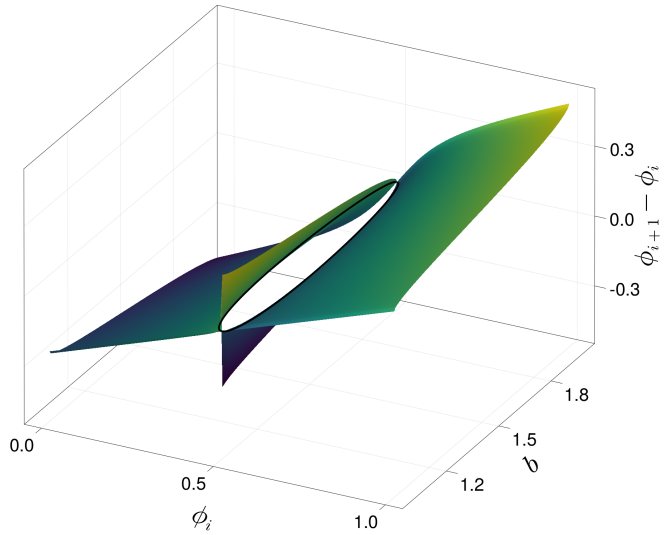

Figure S2. The above surface is Eq.(S17). The black line is Eq.(18) where $\phi_{i+1} = \phi_i$. Eq.(S17) fully intersects Eq.(18) where the period-1 condition ($\phi_{i+1} = \phi_i$) is satisfied.

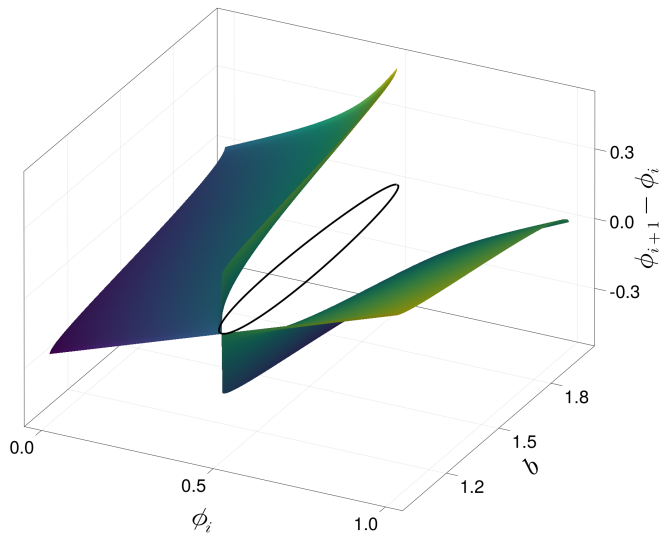

Figure S3. The above surface is Eq.(S18). The black line is Eq.(18) where $\phi_{i+1} = \phi_i$. Eq.(S18) does not intersect Eq.(18) anywhere the period-1 condition ($\phi_{i+1} = \phi_i$) is satisfied.